



Intercellular communication and the organization of simple multicellular animals

P. Japón^{a,b}, F. Jiménez-Morales^{b,*}, F. Casares^{a,*}

^a CABD, GEM-DMC2 Unit (CSIC-Universidad Pablo de Olavide-Junta de Andalucía), 41013 Seville, Spain

^b Department of Condensed Matter Physics, University of Sevilla, 41012 Seville, Spain

ARTICLE INFO

Keywords:

Multicellular organization
Computational models
Swarmalator
Intercellular communication
Self-organization
Decentralized systems

ABSTRACT

Animal cells are amazing examples of decentralized systems: By interchanging information about their position and internal state, cells coordinate their behavior and organize themselves in time and space. Examples of this behavior are the development of an embryo or of an organoid. In this work we have asked which are the “rules of intercellular relationship” that allow the organization of an abstract cell collective into structures similar to simple metazoans, without being specific about the (molecular, cellular or physical) nature of the processes involved. To do so, we have used a computational modeling approach following a modified version of the “Swarmalator” concept introduced by O’Keefe, Hong and Strogatz (2017): a collection of interacting particles (“swarmalators”), each of which defined by a position in space and an internal state (a phase). The key feature is that swarmalators are coupled, so that their position and internal state are both affected by the position and state of all other swarmalators. This model can be easily analogized to biological systems, with “cells” being the swarmalators, and their phase the cell’s internal state or “cell type”. With this model we explore the conditions (represented by the coupling parameters) that would allow the organization of a multicellular “bioswarmer” and its dynamics along a sort of life cycle. Originally developed in 2D, we implement the model in 3D as well. We describe how changing the strength of intercellular communication can alter the structure and differentiation state of the bioswarmer, how internal polarization can arise and trigger collective directed migration, or how partly erasing the cellular memory of cell state is critical to allow bioswarmers to transit through different states. In addition, we show that the size of a multicellular ensemble might control the differentiation of its constituent cells without changing its rules of relationship.

1. Introduction

The first multicellular animals, or “metazoans”, originated about 600 Myrs ago from unicellular protozoans capable of alternating between flagellated and swimming to crawling amoeba-like forms, perhaps similar to modern Choanoflagellates (Brunet and King, 2017; Ros-Rocher et al., 2021). Multicellularity allowed the organization in space of cells with different functional states (“cell types”), in a sort of structured division of labor. The simplest organization includes an external and internal layering of tightly adhered cells, often bearing flagella, called epithelia. The external layer, or ectoderm, forms the outer surface of the organism and often specializes in sensory functions, while the inner layer, or endoderm, forms the digestive cavity or tube. The “in-between” cells are often migratory, phagocytic or contractile. From this simple organization, further cellular specialization and spatial patterning

(“morphogenesis”) have led, through evolution, to all animal forms.

Although in nature this organization develops either from one single cell (the zygote in sexually-reproducing organisms) through multiple divisions, or from a portion of a full organism that then goes on to form a complete animal (in asexually-reproducing organisms), recent work (Simunovic and Brivanlou, 2017) shows how aggregates of stem cells can differentiate in vitro to form multilayered cellular structures, if steered by specific chemical cocktails. These structures, which have been named “embryoids” or “gastruloids”, exhibit remarkable similarities with the proposed organization of early metazoans and reproduce the initial steps in the development of more complex metazoans, including their multilayered organization with the spatial segregation of different cell types (Simunovic and Brivanlou, 2017). These experiments reveal the striking potential for self-organization of animal cells as decentralized systems.

* Corresponding authors.

E-mail addresses: jimenez@us.es (F. Jiménez-Morales), fcasfer@upo.es (F. Casares).

<https://doi.org/10.1016/j.cdev.2021.203726>

Received 20 May 2021; Received in revised form 13 July 2021; Accepted 26 July 2021

Available online 24 August 2021

2667-2901/© 2021 The Authors.

Published by Elsevier B.V. This is an open access article under the CC BY-NC-ND license

(<http://creativecommons.org/licenses/by-nc-nd/4.0/>).

The self-organization of cell collectives relies on intercellular communication. The communicated information must include at least positional information (where a cell is relative to other cells) and identity information (what is the state of other cells). Then, each cell computes these two types of information to define its own location and state accordingly. During normal development, the flow of information between cells and their dynamic responses result in organized functional organisms. In this work we have asked which are the “rules of intercellular relationship” that allow the organization of an abstract cell collective into structures similar to simple metazoans, without being specific about the (molecular, cellular or physical) nature of the processes involved.

2. Results

To find out possible rules of intercellular communication that could result in organized multicellular-like structures, we have used a computational modeling approach following a modified version of the “Swarmalator” concept introduced by O’Keefe et al. (2017). In a collection of particles (“swarmalators”), each of them is defined by a position in space, $\mathbf{x} = (x, y)$ and an internal state (a phase, θ). Swarmalators are coupled, so that their position and internal state are both affected by the position and state of all other swarmalators, being these interactions stronger as the swarmalators are closer. The exploration of the model by varying its coupling parameters revealed a rich set of structures and dynamics (O’Keefe et al., 2017). The swarmalator model can be easily analogized to biological systems, with “cells” being the swarmalators, and their phase, the cells’ internal state or “cell type”. In the original model, attraction and repulsion among swarmalators were both long-range. However, in metazoans, many interactions are short range as they depend on direct cell-to-cell contact or on chemical signals that spread on cellular extensions of limited reach (Gumbiner, 1996). In addition, often these interactions are repulsive, like in the case of cells with different adhesiveness (Foty and Steinberg, 2005) which, when mixed, segregate spatially. Therefore, to make the swarmalator model more akin to multicellular structures, Jiménez-Morales (Jimenez-Morales, 2020) modified the repulsive term, selecting it as a Gaussian function, so that strong repulsion occurs at short distances. The equations of the modified model are:

$$\dot{\mathbf{x}}_i = \frac{1}{N-1} \sum_{j \neq i} (\mathbf{x}_j - \mathbf{x}_i) \left(\frac{1 + J \cos(\theta_j - \theta_i)}{r_{ij}} - \frac{1}{\sigma} e^{-\frac{r_{ij}^2}{\sigma}} \right) \quad (1)$$

$$\dot{\theta}_i = \frac{K}{N-1} \sum_{j \neq i} \frac{\sin(\theta_j - \theta_i)}{r_{ij}} \quad (2)$$

Like in the original model, N is the number of swarmalators (from here on “cells”) and the coupling parameters that indicate the strength of the spatial and phase/cell type interactions are J and K , respectively. r_{ij} denotes the euclidean distance between cells i and j . The repulsive interaction (I_{rep}) is defined as $I_{rep} = \frac{1}{\sigma} e^{-\frac{r_{ij}^2}{\sigma}}$, where σ is a measure of the range of the local interaction.

In what follows we explore the conditions that allow the formation of multicellular-like stable multilayered structures, that we will call “bioswarmers”, and how the coupling among cells and their interaction range affect them, first in 2D, and then in 3D.

2.1. Main parameters and biological analogy

In the model, J affects the intensity of attraction/repulsion between cells depending on how different their state is. In our case, we will consider a general attraction between cells, which promotes their clustering, something that occurs if $0 < J \leq 1$. This phenomenon has been known for a long time since the experiments of H.V. Wilson in which he

showed that dissociated sponge cells would spontaneously reassociate in vitro to form sponge-like structures (Wilson, 1905). This attraction will be maximal for cells with the same state (as $\theta_i = \theta_j \Rightarrow \cos(0) = 1$), which is normally the case in biological systems and is called homotypic interaction. As the term affected (attractive term) by J also depends inversely on the distance between cells, associations among neighbor cells of the same state will tend to be stable. In biological systems, this stability is the result of the establishment of intercellular adhesion (Honig and Shapiro, 2020). σ represents the range and intensity of the repulsive interactions among cells, so that the smaller the σ , the stronger and shorter-range the repulsion. The introduction of this short-range repulsion term (see above) avoids the clumping of cells and their spreading in space. The combination of long-range attraction (“adhesion”) and short-range repulsion (“pushing”) has been recently shown to be important to model the spreading of cell populations (Matsiaka et al., 2019). K controls how strongly cells with different state influence each other. Thus, when $K > 0$ cells tend to have the same state, while if $K < 0$ they tend to have different states (and when $K = 0$ the cells do not respond to the state of others). Here, we have explored the space of structures that arise when $K > 0$, so that cells tend to be of the same phase if they are close to each other. Once we have defined the control parameters (those that control the relationships) of the model, we will investigate which conditions result in structures that mimic some states of a simple, abstracted metazoan.

These are the spatial structuring of cells to form layers, the spatial differentiation of these layers (by their cells acquiring distinct states), the capacity to migrate collectively and the division of the cell collective into two. We first investigate these states separately. However, in biological systems, they are connected into a “life cycle”, so we next determine the changes in the rules of relationship between these bioswarmers that allow the transitions through a simplified life cycle of layering, (reversible) motility, differentiation and division.

In order to observe the motility of the different bioswarmers we introduce the linear momentum ($\mathbf{p} = (p_x, p_y)$) and kinetic energy (T) of a group of cells as a system of particles,

$$T = \frac{1}{2} \sum_i (\dot{x}_i^2 + \dot{y}_i^2) \quad (3)$$

$$\mathbf{p} = m \mathbf{v}_{cm}, \mathbf{v}_{cm} = \frac{\sum_i (\dot{\mathbf{x}}_i + \dot{\mathbf{y}}_i)}{N} \quad (4)$$

where \mathbf{v}_{cm} is the velocity of the center of mass of the group of cells. While the kinetic energy informs about the movement of the bioswarmalators, the linear momentum gives information on the translation movement of the bioswarmer.

2.2. Multilayered structures, motion and cell differentiation

Each experiment is defined by a set of parameters (N, J, K, σ). The initial state (type and position) of the N cells is random. This is the state which implies minimal information. For representation purposes, the phase (θ in Eqs. (1) and (2)) is binned in twelve cell “types” of a different color each ($\theta \in (0, 2\pi]$). Previous work in Jiménez-Morales (2020) had found a region of the parameter space that generated multilayered structures (Fig. 1). This region is the one we explore further in what follows. For simplicity, we set $J = 1$ (i.e. the strength with which cells of different type attract each other is maximal). Therefore, we will identify each experiment as (N, K, σ) , keeping in mind that $J = 1$ always. Fig. 2 shows the final structures resulting for a set of $N = 100$ cells after 6000 time steps. Fig. 2 also includes the values of the kinetic energy (T) and the modulus of momentum (p). Both quantities allow us to discriminate collective displacements of the set and rotations.

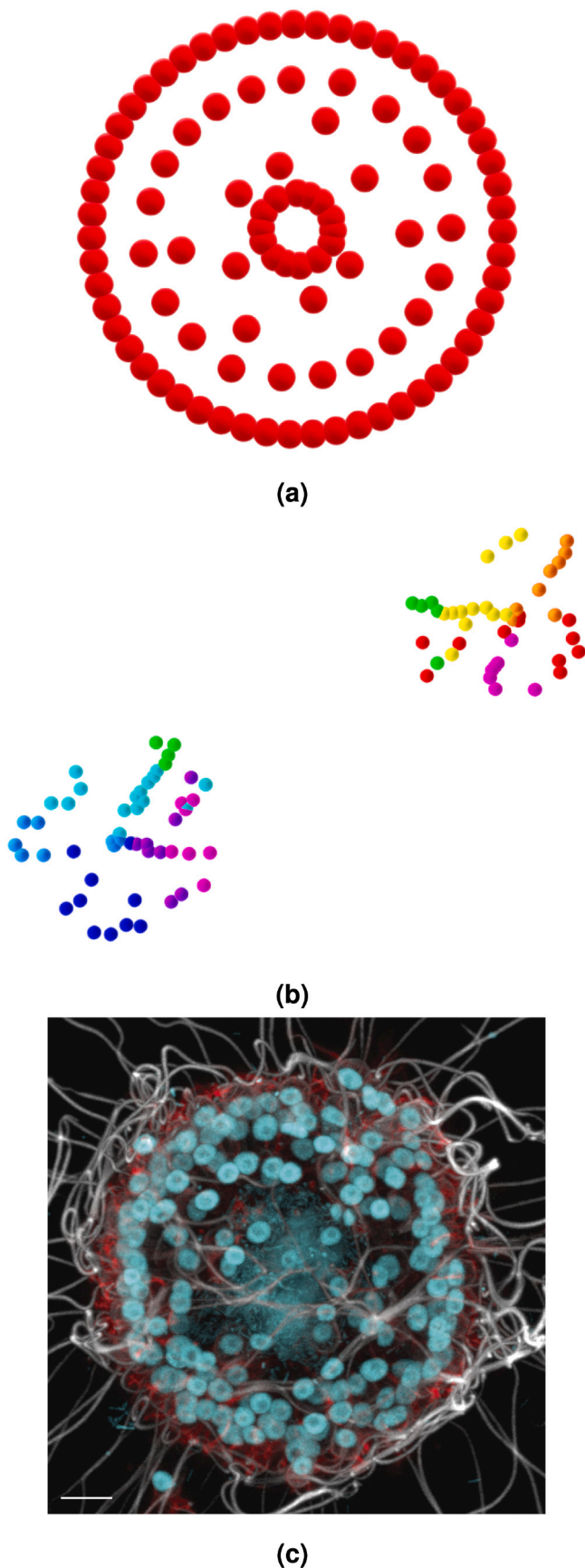


Fig. 1. Closed multilayered structures resembling simple multicellular animals (“bioswarmers”). (a) Structure generated for the set of parameters (100,0.4,0.6) after 6000 time steps. The structure is static and homogeneous with only one cell type. (b) Structure generated for the set of parameters (100,0,0.6) after 6000 time steps. The state is inhomogeneous and dynamic. (c) Confocal image of the choanoflagellate *Salpingoeca monosiera*. The nuclei of the cells are marked in cyan and their motile flagella in white (modified from Hake et al., 2021: <https://www.biorxiv.org/content/10.1101/2021.03.30.437421v1.full>). Courtesy of N. King (University of California, Berkeley, US). Scale bar = 5 μm . (For interpretation of the references to color in this figure legend, the reader is referred to the web version of this article.)

2.3. Directed motion ($K = [0.2, 0.4]$; $\sigma = 0.2$)

For intermediate values of K and σ , bioswarmers form stable, sessile, radially symmetrical multilayered structures (with densely packed outer and inner layers, reminiscent of epithelia, and a more dispersed intermediate layer). These bioswarmers are made up of only one cell state (see Supplementary Video 1) and therefore, they show spatial structure without cell differentiation. At low σ , though, bioswarmers become polarized (with one internal layer defining a “polar” crescent) and motile (e.g. Fig. 2, $K = 0.4$, $\sigma = 0.2$), with the direction of collective motion opposite the crescent (see Supplementary Video 2). As σ reflects the strength of short-range intercellular repulsion, this result implies that the polarization of the structure and its motion arises when this repulsion is not too strong. Most metazoans exhibiting directed motion do show an antero-posterior polarization (i.e. become bilaterally symmetrical). Swarms of the amoeba *Dictyostelium* also aggregate and migrate directed by a source of chemoattractant (reviewed in Kawabe et al., 2019). However, motile bioswarmers show a structural polarity (that is, they are polarized in the absence of an external signal). To understand if the cause of the directed motion is this structural polarity, we removed the internal crescent from motile bioswarmers. These bioswarmers, which lose the bilateral symmetry, stop moving, showing that structural polarization is necessary for directed motion (Fig. 3 and Supplementary Video 3).

2.4. Layer differentiation

The bioswarmers in the central portion of the “morphospace” in Fig. 2 comprise cells of only one cell type. However, besides structural differentiation, metazoans are also composed of different cell types. We see cell type differentiation for $K = 0$ and for $K = 1$. For intermediate and high short-range repulsion (σ belonging to $[0.4, 1.0]$), bioswarmers show clearly differentiated layers (i.e. outer and inner layers made of cells of different types) when the type of a cell is strongly influenced by the state of the swarm (i.e. $K = 1$). Therefore, spatial differentiation required a strong coupling between cells. Interestingly, this bioswarmer state of differentiated layers is dynamic: cells flow from one layer to the other while they change their type constantly, while the overall structure remains stable (see Supplementary Video 4). On the other side of the morphospace, when the phase coupling is inexistent (i.e. $K = 0$) and each cell only responds to the position of the others, and not to their type, the result is the separation of the population into two clusters, akin to reproduction by division (e.g. $\sigma=0.6$) (see Supplementary Video 5).

2.5. “Life cycle”

Metazoans are dynamic structures, and their life histories describe cycles that include division (reproduction), growth, organization and differentiation, motility (e.g. towards nutrients, away from predators or noxious stimuli) and division again. The different stable structures we have described, reached by a coalescent population of cells with random internal states (types) subject to the rules of relationship, could be ordered in a sort of pseudo life-cycle, comprising their structuring, differentiation, (transient) motility and division (Fig. 5). However, can any

(caption on next column)

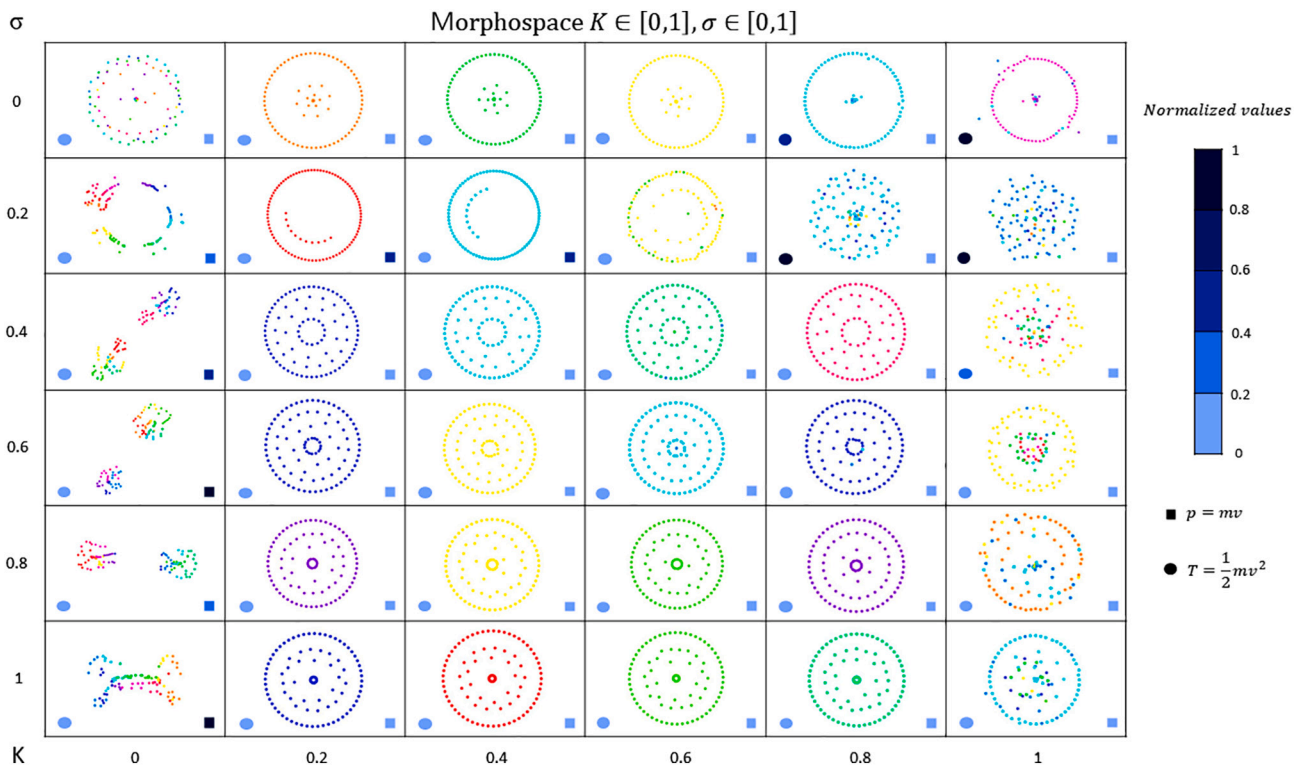


Fig. 2. Two dimensional morphospace $K \in [0,1], \sigma \in [0,1]$. For all structures, $N = 100$. The cell state (phase) is colored as in Fig. 1. The momentum (p) and kinetic energy (T) is also represented. For $K = 0, \sigma \in [0.2, -1]$, the structures rotate. For $K = [0.2, 0.4], \sigma = 0.2$, the structures move coordinately in one direction. Starting from random initial conditions the global characteristics of the final state are the same. For each set of parameters more than 10 runs were made. (For interpretation of the references to color in this figure legend, the reader is referred to the web version of this article.)

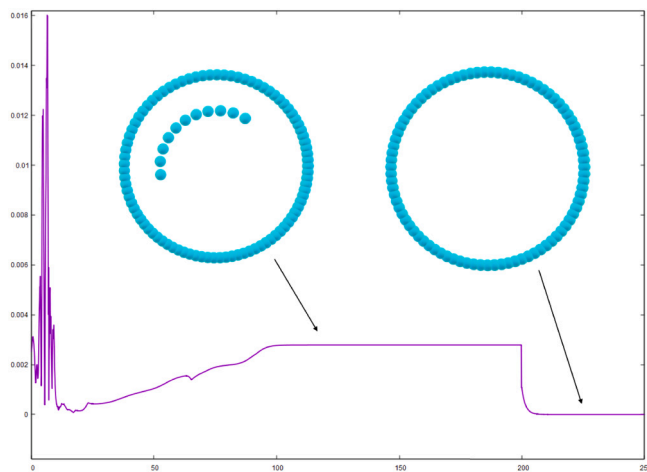


Fig. 3. Linear momentum versus time of the bioswarmer obtained for the set of parameters (100, 0.4, 0.2) starting from a random initial state of cell types. The linear momentum is nearly zero when, at time $t = 25$, the 100 cells with random cell types coalesce. The bioswarmer increases its velocity (center of mass velocity) until it becomes constant. At $t = 200$, the inner crescent cells were removed. Concomitantly, the linear momentum decreases to zero, indicating cessation of movement.

one of these specific structures become another? That is, how can a transition along the “life cycle” be produced? Is it enough to change the ways in which its constituent cells interact -i.e. changing K and σ ?

To explore these questions, we start with a parameter set that results in a multilayered, homogeneous (relative to cell type) and stable state to examine which changes in the control parameters K and σ would allow this state to transit to a new state. The starting bioswarmer (100,0.4,0.6)

is shown in Fig. 4(a). This state is sessile, but it can be readily made motile by reducing σ ($\sigma = 0.2$; Fig. 3). Neither of these states shows internal differentiation - that is, cells in different layers are of the same type. However, adult animals, even if simple in structure, such as sponges or polyps, show spatial differentiation of cell types. Bioswarmers with differentiated cell layers are obtained for values of K close to 1, but starting with a bioswarmer of homogeneous layers (100,0.4,0.6) and changing K to 1 (100,1,0.6) will not make its layers differentiate, simply because there is no cell heterogeneity to start with. However, if we simultaneously set $K = 1$ and randomize the type of a proportion of cells (e.g. 25%). Then the system is led to develop according to the equations. The resulting bioswarmers maintain a multilayered structure but now with spatial cell type differentiation (Fig. 4 (a)). It is important to note that the randomization of type is applied also randomly within the cell population. The final spatial segregation of types occurs as a consequence of the rules of relationship that control the relocation and change of internal state of the cells. This structure can be forced to divide now by “disconnecting” the communication among cells of their type ($K = 0$) and increasing further the percentage of cell type randomization (Fig. 4(b), (100,0.4,0.6) with 75% of random cell types), giving rise to two “daughter” bioswarmers. Finally, each of the daughters could give rise to either a homogeneous or heterogeneous multilayer bioswarmers by reducing its σ and re-establishing the communication of type among the cells ($K > 0$) (Fig. 4(c)). As we have not included cell proliferation (i.e. increase in cell number) in the model, the products of division contain half the number of cells of the parental bioswarmer (Table 1).

2.6. 3D bioswarmers

All the previous experiments showed that 2D bioswarmers exhibit layering, cell differentiation, collective motion and division, all properties of multicellular aggregates/organisms. However, multicellular

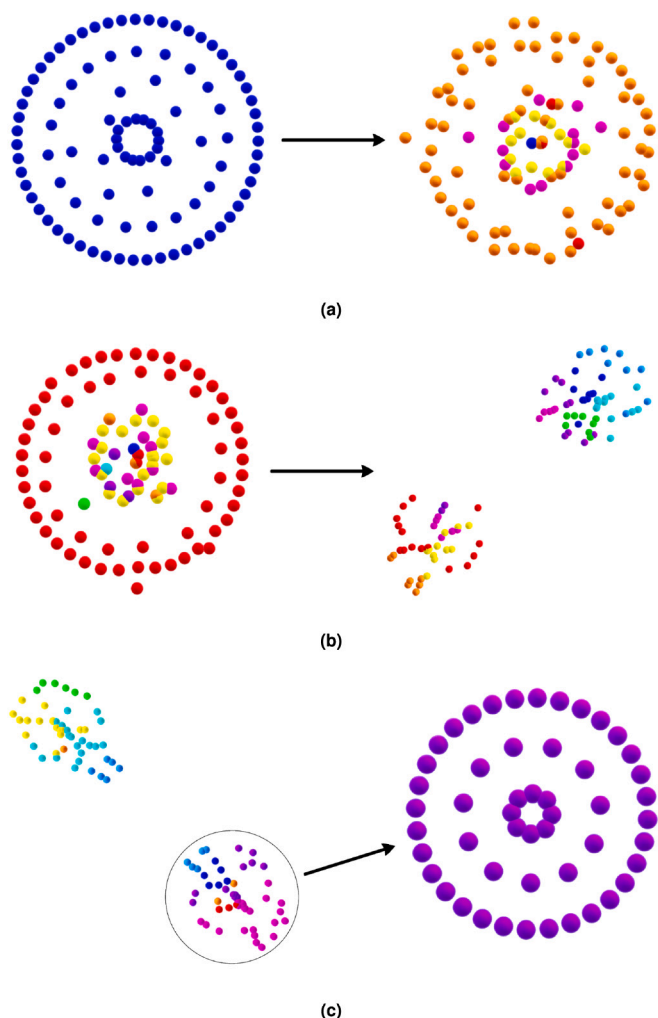


Fig. 4. (a) Generation of a multilayer structure. Starting with a homogeneous bioswarmer obtained for the set of parameters (100,0.4,0.6), 25 cells are randomized and K changes to 1. (b) Cell division. Decreasing K to 0 together with a randomization of 75 cells produces the creation of two entities. (c) Growth and homogenization. Increasing again the parameter K from 0 to 1.

Table 1
Table of experiments summarizing the behaviors of the bioswarmers found for given parameters.

Properties	K	σ	N
<i>2D</i>			
1. Layered organization	[0.2,1]	[0.4,1]	–
2. Motility/polarization	[0.2,0.4]	0.2	–
3. Layered differentiation	[0.8,1]	1	–
<i>3D</i>			
1. Layered organization	1.4	1	–
2. Motility/polarization	1.6	1	–
3. Differentiation threshold	1.4	1	20-25

aggregates/organisms are tri-dimensional. To explore whether bioswarmers could also generate 3D structures akin multicellular organisms we added a third coordinate, so that $\mathbf{x} = (x, y, z)$ through an additional spatial equation as shown in Eq. (1). We find that for values of K around 1,5 and σ around 1, 3D structures with concentric layers showing phase differentiation emerge (Fig. 6), similar to some of the 2D bioswarmers we described above.

Near in the 3D parameter space of K and σ (just increasing K from 1,5 to 1,6), a structure with internal polarization is formed that now starts

collective migration (Fig. 6(b)), again similar to the 2D bioswarmer structure in Fig. 3. Therefore, the transition from a spherical symmetrical to a polarized organization seems to suffice to drive the motion of the whole bioswarmer and this can be achieved by subtle modulations of interaction parameters.

In summary, the extension of the system to 3D results in tridimensional bioswarmers with the same properties than those we described for the simpler 2D bioswarmers, extending our findings to collectives that populate a 3D space.

3. Methods

The mathematical model has been solved using computational methods. Matlab (<https://www.mathworks.com/>) was used for 2D and 3D bioswarmers while Python (<https://www.python.org/>) and Blender (<https://www.blender.org/>) were used for 3D ones for better graphics. The codes are provided as Supplementary material. These codes are commented and therefore provide all information needed for running the program and changing J, K and N parameters as well as calculating the linear momentum or kinematic energy of the cells or making the transitions shown in Fig. 5 in the case of the 2D Matlab code.

4. Discussion

In this paper we have tried to identify general rules of intercellular communication, which we have called “rules of relationship”, among cells that would allow the formation of simple, yet biologically functional, structures. For that, we have used a modification of a computational model, the swarmalator, that generates structures formed by particles which communicate and respond to the two major types of information that guide the development of animal structures: position and internal state (or “cell type”). Although most of the experiments we have carried out were done using bioswarmers in 2D, our preliminary explorations indicate that their behavior in 3D is equivalent. The idea is

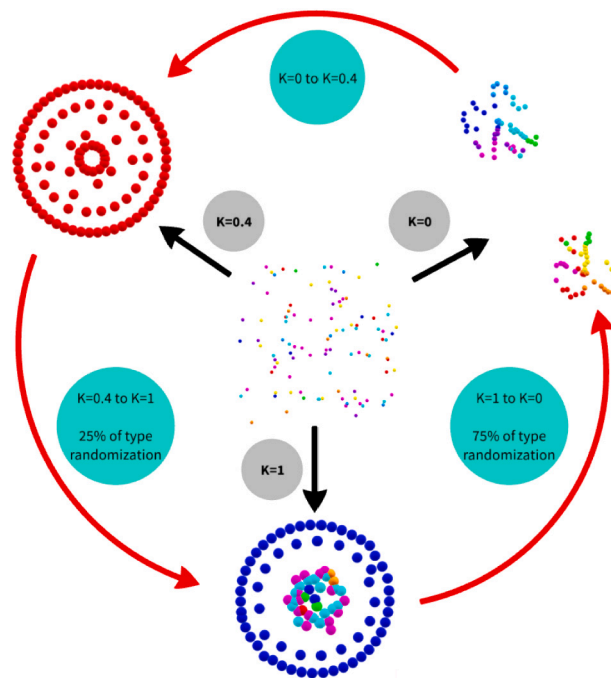


Fig. 5. A coalescing population of “cells” with randomized types (colored) can form a set of different structures depending on the rules of relationship (black arrows). In this diagram, examples of changes in K and in cell-type noise that allow bioswarmers to transit from one structure to another are also indicated (red arrows). (For interpretation of the references to color in this figure legend, the reader is referred to the web version of this article.)

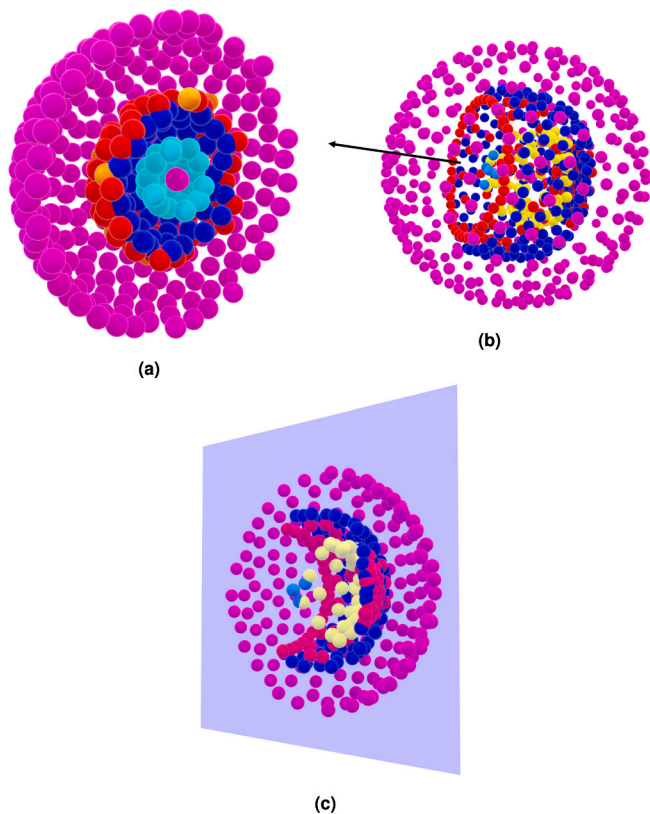


Fig. 6. (a) 3D section of structures with $N = 800$ where concentric layers with cell differentiation are seen (800,1.4,1). Whole structure (b) and section (c) of (800,1.6,1). This bioswarmer moves in a certain direction (black arrow in (b)) due to its axial symmetry. The spherical symmetry seen before in (a), turns into axial symmetry changing K from 1.4 to 1.6, resulting in a motile structure.

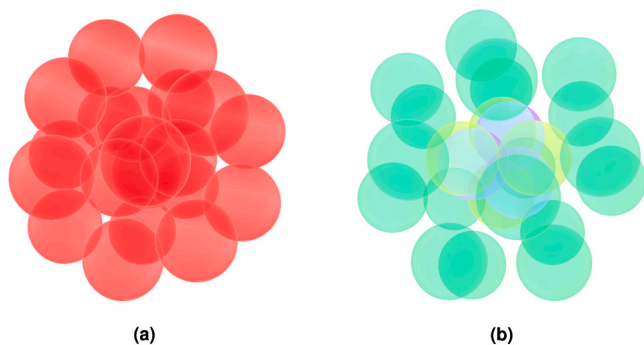


Fig. 7. The number creates a cell differentiation. (a) At a low number of cells ($N = 20$) in 3D every cells are of the same type. The set of parameters is (20,1.4,1); (b) cell differentiation is obtained when a threshold is exceeded. In this case $N = 25$.

that, even accepting that this is an exceedingly simplified model, some fundamental rules may arise. The first conclusion is that even if the short-range repulsion term is negligible (i.e. $\sigma = 0$) bioswarms are able to form stable structures with an outer layer. However, further internal layering occurs when σ increases, indicating that short-range repulsion helps increase their structural complexity. One special case is motility. In the transition between sessile structures, increase of σ causes the structural reorganization of the bioswarms from radial (or spherical) symmetry to bilateral symmetry –that is, an antero-posterior axis emerges. In animal systems, collective migration is characterized by a front-rear polarity of the moving cell group (Friedl and Gilmour, 2009).

Often, the moving group shows some internal cell differentiation, so that “leading” or “tip” cells specialize at the front of the migrating group (Friedl and Gilmour, 2009). In the case of motile bioswarms, though, the directional collective motion is not the result of polarized cell differentiation, as the motile 2D forms have homogeneous cell types, but emerges from a polarization of its structure, something that has been named “supra-cellular polarity” (Shellard et al., 2018). We have shown that the polarized segregation of an internal cell crescent endows bioswarms with polarity and this results in directed motion. The intercellular attraction maintains the structure as it migrates. Therefore, our results suggest that directed collective migration may arise without the need of polarized cell differentiation. Indeed, the generation of specialized leading or tip cells for collective migration might not be a general rule: for example, the migration of mammary duct cells during the development of the gland seems to proceed without specialized leading cells (Ewald et al., 2008). It is interesting to note that only when cells show some degree of intercellular repulsion collective motility starts. A recent paper has experimentally tested precisely this. An in vitro assembled epithelium subject to an electric field will not move unless the strength of the intercellular adhesive links is weakened. Only when this experimental weakening is induced (equivalent to cells exerting slight short-range repulsion among them) the cells migrate collectively under the influence of the electric field, following, in this real biology case, the direction marked by this field (Shim et al., 2021). One interesting aspect of migration initiation seems to be the degree of cohesiveness among the cell collective. For example, neural crest cells, a cell type derived from the neural tube that migrates away from this epithelial tube to form diverse bones, cartilages or nerves, start migrating when reducing the strength of their intercellular links, which allows a transition from an epithelial structure, in which cells are tightly linked, to a mesenchymal state where cells, although cohesive, can reorganize and migrate. A small increase in σ should result in a similar weakening in the short-range attraction between bioswarms as well as in their local repulsion. In fact, recent work showed that the migration of neural crest cell collectives derived from a phenomenon called CIL: Contact inhibition of locomotion, by which cells that get in contact move away from each other (Li et al., 2019; Roycroft et al., 2018) – that is, undergo a short-range repulsion- suggesting that this tad of short-range repulsion might be a general rule that allows collective migration.

Multilayered bioswarms are often static and homogeneous. Although their structural layering might offer them some possibility for functional specialization, multicellular organization relies on the spatial structuring of different cell types. Within the parameter subspace we have explored, this happens when the information on cell type strongly affects the cell's own type. These bioswarms are sessile (their center of mass remains unchanged) but are internally dynamic: cells can move from one layer to another as they change their type and yet, the structure is maintained in this quasi-stable cell state. This type of bioswarms is most interesting, as they recapitulate internal cell migrations and changes in cell type that are seen during the development and maintenance of organs and organisms. Reaching this bioswarmer state from other (e.g. the static, multilayered and homogeneous) requires some degree of randomization of the cell state. Randomization of cell types is equivalent to a partial loss of memory of cell states in the system. Our experiments indicate that structural plasticity requires this memory loss. The extreme case is seen when the bioswarmer “divides”. This only happens when noise is maximal, together with loss of intercellular communication of cell type information. This situation, in which cells lose track of their past state, is equivalent to a “loss of epigenetic memory” similar to that described for newly formed zygotes (Eckersley-Maslin et al., 2018) or for induced pluripotent stem cells (Van den Hurk et al., 2016). These conclusions derive from the study of 2D bioswarms. 3D bioswarms, though, can organize themselves into more complex structures: e.g. Under certain parameter sets, 3D bioswarms can be multilayered, with cell type differentiation, exhibit internal polarization and show collective motion (Fig. 7). Our exploration of the

parameter space has not been so thorough as to rule out this sort of complex bioswarmers in 2D but it might be that adding an additional dimension (and becoming more realistic) confers bioswarmers also additional organizational possibilities. One last aspect that might influence the capacity of a multicellular collective to organize into cell-differentiated cellular layers is its size - i.e. the number of its constituent cells. A recent work has investigated the influence of cell number on the differentiation of cells coupled through intercellular signaling (Stanoev et al., 2021). In this investigation, the cell type is determined by a toggle-switch-like network with negative feedback (one of the types produces a signal that represses this type), in which the feedback signal is precisely the coupling signal as well. The key finding, using these model, is that the transition of the cell collective from an undifferentiated state to one in which the population splits into cells of either one of the two types depends on cell number -that is, differentiation only occurs above a certain cell number threshold (Stanoev et al., 2021). We explored whether a size-dependence in cell differentiation may also be at work in our bioswarmers. Indeed, two 3D bioswarmers, with identical parameters and only differing in their cell number showed that while the small one ($N = 20$) does not differentiate, already increasing its N to 25 cells results in differentiation (Fig. 7). Although needing a systematic investigation of the effect that size (cell number) has on the differentiation capacity of bioswarmers, this preliminary experiment suggests bioswarmer's size is also a critical variable in a system where there are no negative feedbacks.

Globally, the study of bioswarmers has identified potential ways in which modulating intercellular interactions among coupled cells might drive the formation of simple metazoan-like structures, and how these modulations, together with some information loss of cell state, can make these structures transit through a simple life cycle. Compared with previous work using swarmalators, our work has focused on the specific subspace of coupling parameters that result in simple metazoan-like structures. Exploiting this analogy, we have found that modulation in the strength of two of these parameters (which control the intensity with which cell fate is controlled by the fate of surrounding cells as well as the intensity of short-range intercellular repulsion) results in layered structures that may exhibit directed collective motility, cellular “differentiation” and are even able to split as in a reproductive process. Interestingly, the transition between some of these states (that resemble the transitions through an animal's life cycle) require that a fraction of its constituent cells lose its cell fate -something loosely analogous to an epigenetic erasure of cell type information. Still, there are a number of questions that need follow-up investigation. As mentioned above, a detailed study of how cell number affects the differentiation of cells states is required. In this regard, our system does not include cell proliferation, a key ingredient in biological systems. The implementation of the system in 3D we have performed should allow further exploration of bioswarmer structures with a more realistic structure. Also, including noise will make bioswarmers more akin biological systems -where some degree of noise, both internal as well as external, is unavoidable. And lastly, the short-range repulsive relationships have been modeled using a particular function. Using other functions to more accurately describe intercellular interactions (such as those mediated by intercellular ion channels (Prindle et al., 2015), or those triggered during nerve impulse transmission) might result in an enriched set of structures and the possibility of studying their relevance to biological multicellular systems.

Supplementary data to this article can be found online at <https://doi.org/10.1016/j.cdev.2021.203726>.

CRediT authorship contribution statement

FJ-M and FC conceived the project. PJ and FJ-M wrote the code and run the computational experiments. PJ and FC prepared the figures and wrote the manuscript draft. PJ, FJ-M and FC analyzed results and participated in the writing of the final manuscript.

Acknowledgments

Python code for Blender made by Julia F. Ereza (IAA-CSIC).

Funding

Grants PGC2018-474 093704-B-I00 and MDM-2016-0687, from MINECO (Spain) cofunded by FEDER, to FC.

Funding for open access publishing

Universidad Pablo de Olavide/CBUA.

References

- Brunet, T., King, N., 2017. The origin of animal multicellularity and cell differentiation. *Dev. Cell* 43, 124–140.
- Eckersley-Maslin, M.A., Alda-Catalinas, C., Reik, W., 2018. Dynamics of the epigenetic landscape during the maternal-to-zygotic transition. *Nat. Rev. Mol. Cell Biol.* 19, 436–450.
- Ewald, A.J., Brenot, A., Duong, M., Chan, B.S., Werb, Z., 2008. Collective epithelial migration and cell rearrangements drive mammary branching morphogenesis. *Dev. Cell* 14, 570–581.
- Foty, R.A., Steinberg, M.S., 2005. The differential adhesion hypothesis: a direct evaluation. *Dev. Biol.* 278, 255–263.
- Friedl, P., Gilmour, D., 2009. Collective cell migration in morphogenesis, regeneration and cancer. *Nat. Rev. Mol. Cell Biol.* 10, 445–457.
- Gumbiner, B.M., 1996. Cell adhesion: the molecular basis of tissue architecture and morphogenesis. *Cell* 84, 345–357.
- Honig, B., Shapiro, L., 2020. Adhesion protein structure, molecular affinities, and principles of cell-cell recognition. *Cell* 181, 520–535.
- Jimenez-Morales, F., 2020. Oscillatory behavior in a system of swarmalators with a short-range repulsive interaction. *Phys. Rev. E* 101, 062202.
- Kawabe, Y., Du, Q., Schilde, C., Schaap, P., 2019. Evolution of multicellularity in dictyostelia. *Int. J. Dev. Biol.* 63, 359–369.
- Li, Yuwei, Vieceli, F.M., Gonzalez, W., G. A., Li, 2019. In vivo quantitative imaging provides insights into trunk neural crest migration. *Cell Rep* 26 (6), 1489–1500.
- Matsiaka, O.M., Baker, R.E., Shah, E.T., Simpson, M.J., 2019. In: *Mechanistic and Experimental Models of Cell Migration Reveal the Importance of Cell-to-Cell Pushing in Cell Invasion*. Express, Biomed. Phys. Eng, p. 5.
- O’Keeffe, K.P., Hong, H., Strogatz, S.H., 2017. Oscillators that sync and swarm. *Nat. Commun.* 8, 1504.
- Prindle, A., Liu, J., Asally, M., Ly, S., García-Ojalvo, J., Süel, G.M., 2015. Ion channels enable electrical communication in bacterial communities. *Nature* 527, 59–63.
- Ros-Rocher, N., Perez-Posada, A., Leger, M.M., Ruiz-Trillo, I., 2021. The origin of animals: an ancestral reconstruction of the unicellular-to-multicellular transition. *Open Biol.* 11, 200359.
- Roycroft, A., Szabó, A., Bahm, I., Daly, L., Charras, G., Parsons, M., Mayor, R., 2018. Redistribution of adhesive forces through Src/FAK drives contact inhibition of locomotion in neural crest. *Dev. Cell* 45 (5), 565–579.
- Shellard, A., Szabó, A., Trepast, X., Mayor, R., 2018. Supracellular contraction at the rear of neural crest cell groups drives collective chemotaxis. *Science* 362, 339–343.
- Shim, G., Davenport, D., Cohen, D.J., 2021. Cellular crowd control: overriding endogenous cell coordination makes cell migration more susceptible to external programming. *bioRxiv*. <https://doi.org/10.1101/2021.01.23.427700>.
- Simunovic, M., Brivanlou, A.H., 2017. Embryoids, organoids and gastruloids: new approaches to understanding embryogenesis. *Development* 144, 976–985.
- Stanoev, A., Schroter, C., Koseska, A., 2021. Robustness and timing of cellular differentiation through population-based symmetry breaking. *Development* 148.
- Van den Hurk, M., Kenis, G., Bardy, C., van den Hove, D.L., Gage, F.H., Steinbusch, H.W., Rutten, B.P., 2016. Transcriptional and epigenetic mechanisms of cellular reprogramming to induced pluripotency. *Epigenomics* 8, 1131–1149.
- Wilson, H.V., 1905. On some phenomena of coalescence and regeneration in sponges. *J. Exp. Zool.* 5, 245–258.